

Dimethyl Fumarate Inhibits the Nuclear Factor κB Pathway in Breast Cancer Cells by Covalent Modification of p65\*

Irida Kastrati<sup>1</sup>, Marton A. Siklos<sup>2</sup>, Esther L. Calderon-Gierszal<sup>1</sup>, Lamiaa El-Shennawy<sup>1</sup>, Gergana Georgieva<sup>1</sup>, Emily N. Thayer<sup>2</sup>, Gregory R. J. Thatcher<sup>2</sup>, and Jonna Frasor<sup>1</sup>

<sup>1</sup>From the Department of Physiology and Biophysics,

<sup>2</sup>Department of Medicinal Chemistry and Pharmacognosy  
University of Illinois at Chicago, Chicago, IL 60612, USA

\*Running title: *Anti-NFκB activity of DMF in breast cancer cells*

To whom correspondence should be addressed: Irida Kastrati, Department of Physiology and Biophysics, University of Illinois at Chicago, 835 S. Wolcott Ave., E202 MSB, MC901, Chicago, IL, 60612, USA, Tel.: (312) 355-2578; Fax: (312) 996-1414; E-mail: ikastr2@uic.edu

**Keywords:** Breast cancer; cysteine 38; covalent modification; dimethyl fumarate; drug; inflammation; inhibitor; NFκB; mammospheres.

---

**ABSTRACT**

In breast tumors, activation of the nuclear factor κB (NFκB) pathway promotes survival, migration, invasion, angiogenesis, stem cell-like properties, and resistance to therapy – all phenotypes of aggressive disease where therapy options remain limited. Adding an anti-inflammatory/anti-NFκB agent to breast cancer treatment would be beneficial, but no such drug is approved as either a mono- or adjuvant therapy. To address this need, we examined whether dimethyl fumarate (DMF), an anti-inflammatory drug already in clinical use for multiple sclerosis, can inhibit the NFκB pathway. We find that DMF effectively blocks NFκB activity in multiple breast cancer cell lines and abrogates NFκB-dependent mammosphere formation, indicating that DMF has anti-cancer stem cells properties. In addition, DMF inhibits cell proliferation and significantly impairs xenograft tumor growth. Mechanistically, DMF prevents p65 nuclear translocation and attenuates its DNA binding activity, but has no effect on upstream proteins in the NFκB pathway. Dimethyl succinate (DMS), the inactive analog of DMF that lacks the electrophilic double bond of fumarate, is unable to inhibit NFκB activity. Also, the cell permeable thiol, N-acetyl L-cysteine, reverses

DMF's inhibition of the NFκB pathway, supporting the notion that the electrophile, DMF, acts via covalent modification. To determine whether DMF directly interacts with p65, we synthesized and used a novel chemical probe of DMF by incorporating an alkyne functionality, and found that DMF covalently modifies p65 with cysteine 38 being essential for DMF's activity. These results establish DMF as an NFκB inhibitor with anti-tumor activity that may add therapeutic value in treating aggressive breast cancers.

---

In the US, breast cancer is the second most prevalent cancer among women and claims over 40,000 lives each year. Despite major advancements in breast cancer treatment, successful therapy outcome is limited to early detection of cancer at the primary organ. Therapy options for aggressive breast cancer disease (i.e. advanced stage, therapy-resistant, recurrent, or metastatic) are limited. As a result, prognosis remains poor and aggressive disease accounts for over 90% of breast cancer related deaths.

Although the underlying mechanisms are not fully understood, inflammation has emerged as a key instigator and driver of aggressive breast cancers (1,2). More specifically, the nuclear factor κB (NFκB) pathway promotes multiple aggressive

tumor phenotypes including cell survival, migration, invasion, angiogenesis and resistance to therapy (3,4). The link between the inflammatory NFκB pathway and breast cancer is also supported by the fact that a deregulated, or constitutively active NFκB pathway is associated with aggressive breast cancer phenotypes and therapy resistance (5-9). More recently, activation of the NFκB pathway has been shown to regulate the survival and propagation of breast cancer stem cells (CSCs) (10-12), which are a small subset of tumor cells, that evade all standard therapies and are involved in metastasis and tumor recurrence (13-18). Given that the NFκB pathway is essential for breast cancer progression and aggressiveness, its inhibition can be exploited to eradicate CSCs and other detrimental NFκB-dependent tumor phenotypes. Yet, to date, there are no such NFκB pathway inhibitors available in the clinic.

Therapeutic targeting of the NFκB activity has been directed at inhibiting various players in the pathway (19). The canonical NFκB pathway consists of p65 (RelA) and p50 transcription factors, which are held in the cytoplasm by an inhibitor protein, IκBα. Upon stimulation by inflammatory cytokines, such as TNFα, IL-1β or other factors, the IκB kinase (IKK) complex, consisting of IKKα, IKKβ and the scaffolding protein NEMO, is activated. This leads to phosphorylation and proteasomal degradation of IκBα. As a result, p65/p50 factors are liberated and can translocate to the nucleus, where they bind to DNA and induce gene transcription (20). Therefore, inhibitors targeting the proteasome and upstream kinases have been investigated as a new class of anti-inflammatory drugs, but most have failed due to inhibition of other non-NFκB targets and toxic side effects (21). In addition, given that NFκB is also critical to the innate immune system, most NFκB inhibitors display long-lasting immune suppression. As a result, development of safe NFκB inhibitors is even more challenging (22), especially for anti-cancer therapy where continued inhibitor use is required. This raises the issue on how to safely and effectively inhibit the NFκB pathway. One option is to use the anti-inflammatory drug Tecfidera (dimethyl fumarate, DMF). DMF was approved in the US in March 2013 for multiple sclerosis and is now the number one prescribed oral therapy for relapsing forms of the disease. DMF is neuroprotective and is

proposed to act via inhibition of NFκB and activation of Nrf2 pathways (23-26). Most importantly, DMF has a proven safety in humans – it has immune-modulatory properties without significant immune suppression (27). This makes DMF an attractive candidate for NFκB inhibition. Moreover, its therapeutic potential in breast cancer therapy has yet to be explored.

Our studies indicate that DMF inhibits NFκB activity in multiple breast cancer cell lines. Consistent with its anti-NFκB activity, DMF also inhibits mammosphere (MS) formation, cell proliferation and xenograft tumor growth. Mechanistically, we find that DMF covalently modifies the NFκB transcription factor, p65, to block its nuclear translocation and DNA binding activity. These results provide proof-of-principle evidence that DMF can be used to inhibit NFκB activity in breast cancer cells. Understanding DMF's mechanism of action could provide the needed rationale to advance DMF into the clinic for aggressive breast cancer therapy.

## **EXPERIMENTAL PROCEDURES**

*Reagents* – TNFα was purchased from R&D Systems. DMF, DMS, NAC and methyl cellulose were purchased from Sigma. IKK7 was purchased from EMD Millipore. Compound 16 was obtained from Dr. Terry Moore (University of Illinois at Chicago). DAPI, ProLong Gold antifade reagent, protein A dynabeads, and streptavidin M-280 dynabeads were purchased from Invitrogen. Click chemistry reagents tris(2-carboxyethyl)phosphine (TCEP), carboxyrhodamine 110-azide, and biotin-PEG3-azide were purchased from Click Chemistry Tools. Antibodies for p-IKKα/β (#2697), IKKα (#2682), IKKβ (#2370), p-IκBα (#2859), IκBα (#4814), p-p65 S536, (#3033), p-p65 S468, (#3039), and TBP (#8515) were purchased from Cell Signaling. The antibody for p65 (sc-372) was purchased from Santa Cruz. The antibody for β-actin (A5441) was purchased from Sigma. The Alexa Fluor 594 conjugated goat anti-Rabbit antibody (A11012) was purchased from Invitrogen.

*DMF Probe Synthesis* – DMF probe was synthesized as previously described in the literature by Gotz et al. (28).

*Cell Lines and Culture Conditions* – Human estrogen receptor (ER) positive breast cancer cell lines, MCF-7 and T47D, and the

ER+/Her2+ cell line, BT474, were obtained from Dr. Debra Tonetti (University of Illinois at Chicago). Constitutively active IKKβ (CA-IKKβ) cells are stably transfected MCF-7 cells engineered to overexpress a doxycycline (Dox)/tetracycline-inducible, constitutively active form of IKKβ (S177E / S181E) (29). Briefly, cells were derived using the Retro-X Tet-On Advanced Inducible Expression System from Clontech. The IKKβ expression vector was purchased from InvivoGen. Mutations were introduced using site-directed mutagenesis (Stratagene), and the CA-IKKβ plasmid was then subcloned into the puromycin resistant Tet-On vector, pRetroX-Tight-Pur. Retrovirus generation and infection of MCF-7-rtTA cells, which were stably transduced with a geneticin-resistant vector encoding the Tet-activator rtTA, were performed according to previously published protocol (30). Single cell clones were selected using geneticin and puromycin and fully characterized for NFκB activity (data not shown). MCF-7, T47D, BT474 and CA-IKKβ cells were routinely maintained in RPMI 1640 media (Invitrogen Life Technologies) with phenol red supplemented with 10% FBS, 1% non-essential amino acids, 2mmol/L L-glutamine, 1% antibiotics penicillin-streptomycin, and 6ng/mL insulin. The ER- breast cancer cell line, MDA-MB-231, was obtained from Dr. Clodia Osipo (Loyola University Chicago) and routinely maintained in IMEM media (Corning) supplemented with 5% FBS, 1% non-essential amino acids, 2mM L-glutamine, and 1% antibiotics penicillin-streptomycin.

*Luciferase Reporter Assay* – MCF-7 cells were transiently co-transfected with an NFκB-RE luciferase construct (Clontech) along with the renilla luciferase construct, pGL4.70 (Promega), and dual luciferase assays were carried out as previously described (31). The mammalian expression vectors containing cDNAs for wild type p65 and mutant C38S-p65 were a generous gift from Dr. Thomas Gilmore (Boston University) and have been previously described in detail (32).

*RT-Quantitative PCR (QPCR)* – RNA isolation was carried out using Trizol according to the manufacturer's instructions (Invitrogen). Total RNA (0.5 μg) was reverse transcribed using Moloney murine leukemia virus reverse transcriptase (Invitrogen). The resulting product was diluted to 100 μL with double-distilled water

and 2 μL were used for each subsequent quantitative PCR reaction. Quantitative PCR was carried out and analyzed as previously described (33). All QPCR primers used were validated and previously reported (33). Fold change was calculated using the  $\Delta\Delta C_t$  method with ribosomal protein 36B4 mRNA serving as the internal control.

*Mammosphere (MS) Assay* – Breast cancer cells were seeded at single cell density on low attachment plates in media described by Dontu et al., supplemented with 1% methyl cellulose to prevent cellular aggregation (27). After 7 days, the diameter of MS was measured and MS  $\geq 75\mu\text{m}$  in diameter were counted. For MS formation studies, inhibitors were added the day after seeding. For RNA, p65 DNA binding activity, and protein studies, MS were grown for 7 days and inhibitors were added for the last 3-6 hours.

*Crystal Violet Proliferation Assay* – Briefly, cells were seeded in 24-well plates and treated for 7 days with varying concentrations of DMF. Cells were then stained with crystal violet (0.5% in 20% methanol) for 15 minutes, solubilized using 1% sodium dodecyl sulfate solution, and an absorbance reading was taken at 570 nm.

*Xenograft Study* – All mouse experiments were carried out at the University of Illinois at Chicago animal facility. All mouse experiments were conducted in accordance with institutional procedures and guidelines, and prior approval from the Institutional Animal Care and Use Committee. Female athymic nude mice (nu/nu), aged 4-5 week-old, were purchased from Harlan. Five million MDA-MB-231 cells were injected orthotopically into the thoracic mammary glands (N =14-16 injections per group). Tumor formation was monitored by palpation and once tumors were detected, mice were randomized into either vehicle control or DMF groups. Mice were gavaged daily with vehicle (0.8% methyl cellulose) or DMF (30mg/kg, suspended in 0.8% methyl cellulose). Tumor sizes were measured daily with an electronic caliper and tumor volume was calculated as  $(\text{length} \times \text{width}^2) \times \pi/2$ . Tumor growth was monitored until total tumor burden reached humane end-point criteria.

*p65 DNA Binding Assay* – p65 DNA binding activity of nuclear proteins extracted from

MCF-7 cells, or of recombinant p65 protein (31102, Active Motif) was measured via an ELISA (Active Motif) according to manufacturer's guidelines.

**Chromatin Immunoprecipitation (ChIP) assay** – ChIP assay was performed as previously described with some modifications (34). Briefly, MCF-7 cells were crosslinked with 2mM disuccinimidyl glutarate followed by 1% formaldehyde. For the precipitations, beads were coated with antibody prior to pulldown and pulldowns occurred while rotating for 16 hours at 4°C. Beads were then washed with TSE I (20mM Tris/HCl, 150mM NaCl, 0.1% SDS, 1% Triton X-100, 2mM EDTA), twice with TSE III (10mM Tris/HCl, 250mM LiCl, 1% IGEPAL CA-630, 0.7% Deoxycholate, 1mM EDTA), and twice with TE followed by elution from the beads using elution buffer (0.1M NaHCO<sub>3</sub>, 1% SDS). Elutions were subsequently de-crosslinked overnight at 65°C and DNA was purified and used for QPCR. QPCR primer sequences are available upon request.

**Western Blot** – Whole cell extracts were prepared using the M-PER reagent (Thermo Scientific). Proteins are separated by SDS-PAGE (Bio-Rad Laboratories), transferred to nitrocellulose membranes (Thermo Scientific), blocked for 1 hour in buffer containing 5% nonfat dry milk (Lab Scientific) or 5% bovine serum albumin, and incubated with the appropriate primary antibody overnight. The next day, secondary antibody was applied and the signal was visualized on a Molecular Imager ChemidocXRS (Bio-Rad Laboratories) using the Pierce Supersignal West Pico chemiluminescent substrate (Thermo Scientific). Images were obtained using Quantity One software (Bio-Rad Laboratories).

**Immunohistochemistry (IHC)** – Cells were seeded on 0.1% gelatin coated coverslips. After treatment, cells were fixed with 4% para-formaldehyde for 10 minutes, permeabilized using 0.1% Triton X-100 for 1 minute, and blocked with 10% serum in PBS for 1 hour. Cells were then stained overnight at 4°C with the p65 antibody (dilution 1:200), followed by 1 hour incubation with the Alexa Fluor 594 conjugated secondary antibody (dilution 1:1000). The coverslips were mounted with ProLong Gold antifade reagent with DAPI. Images were then acquired at 63X

magnification using the LSM710 confocal microscope.

**In-Gel Fluorescence** – In situ labelled recombinant p65 protein and its in-gel fluorescence activity was measured as previously described with some modifications (35). Briefly, p65 protein, with or without pre-incubation with 50μM DMF for 30 minutes, was reacted with DMF probe (50μM) at 37°C for 30 minutes. After click chemistry reaction (36) using CuSO<sub>4</sub>, TCEP, and carboxyrhodamine 110-azide, the rhodamine labelled p65 protein was separated by SDS-PAGE. The gel was then visualized by in-gel fluorescence scanning using the Typhoon system and is shown in a gray scale.

**Immunoprecipitation** – MDA-MB-231 cells were lysed using RIPA buffer and the lysate was purified using a 10kDa cutoff Millipore Amicon column. Samples containing about 500μg of total protein were reacted with DMF probe or vehicle control (DMSO) as described above. Click chemistry was performed on the samples using CuSO<sub>4</sub>, TCEP, and biotin-PEG3-azide. Biotinylated proteins were incubated with streptavidin beads and pulldown occurred while rotating for 30 minutes at room temperature. Beads were then washed twice with PBS, and proteins are eluted with 0.1% SDS at 95°C for 5 minutes.

**Statistical Analysis** – Data are presented as mean ± SEM from at least three independent determinations. Statistical analysis consisted of 1- or 2-way ANOVA followed by Tukey posttest, or *t* test, as appropriate.

## **RESULTS**

**Anti-NFκB Activity of DMF in Breast Cancer Cells** – To determine whether DMF inhibits the NFκB pathway in breast cancer cells, we measured DMF's activity on several NFκB endpoints (Fig. 1A-D). Following TNFα-induced activation of the NFκB pathway, we find that DMF inhibits both NFκB-RE activity (Fig. 1A) and expression of NFκB target genes, such as CCL2 and TNF (Fig. 1B-D), in a dose-dependent manner with a calculated IC<sub>50</sub> value of ~20μM. Moreover, DMF's inhibitory effect is shown in three different breast cancer cell lines, MCF-7, BT474 and MDA-MB-231 cells, representing different breast cancer subtypes: estrogen receptor

positive, Her2 positive and triple negative subtype, respectively. In an alternative non-cytokine induced model, we tested DMF's activity in the stably transfected MCF-7 cells with constitutively active IKKβ (CA-IKKβ), a key kinase in the NFκB pathway. Upon adding doxycycline (Dox), the NFκB pathway is activated as shown by elevated target gene expression (Fig. 1E). Similar to cytokine-induced activation of NFκB, we find that adding DMF blocks Dox-induced gene expression in the CA-IKKβ cells in a dose-dependent manner (Fig. 1F). Therefore, DMF inhibits NFκB activity across multiple breast cancer cell lines under various stimuli that activate NFκB pathway. To test the effect of DMF on other transcription factors, we chose the estrogen receptor given its prominent role in breast cancer. We find that DMF, 20μM, has no effect on classical estrogen receptor-target genes, such as TFF1 and IGFBP4, shown in Fig. 1G. This suggests that DMF does not exert a general non-specific effect on transcription factors in breast cancer cells.

*DMF Inhibits Cell Proliferation, MS Formation and Xenograft Tumor Growth* – Given that breast CSCs survival and propagation has been shown to be dependent on NFκB activity (10-12), we next explored whether DMF could affect formation of MS, which are enriched for cells with the stem cell-like properties of self-renewal and anchorage-independent growth (37,38). Two NFκB pathway inhibitors, IKK7 and Bay117082, were used as controls (Fig. 2B) on MS formation. Similar to the known NFκB inhibitors, we find that DMF abrogates MS formation in a dose-dependent manner in all breast cancer cell lines examined (Fig. 2A solid line, 2B). IC<sub>50</sub> values for MS inhibition across the different cell lines is ~20μM, the same IC<sub>50</sub> values observed for inhibition of cytokine-induced NFκB pathway in adherent monolayer cultures.

At similar potency to inhibition of the NFκB pathway and MS formation, DMF acted to inhibit cancer cell proliferation as measured by the crystal violet assay (Fig. 2A dashed line). These in vitro effects of DMF prompted us to examine DMF's activity on xenograft tumor growth. We find that DMF (30mg/kg daily) significantly impairs MDA-MB-231 tumor growth in athymic nude mice (Fig. 3C) without affecting animal weights (data not shown). Together, these data

indicate, for the first time, the efficacy of DMF on breast cancer phenotypes both in vitro and in vivo.

*DMF Inhibits the High Intrinsic NFκB Activity in MS* – To determine if DMF inhibits NFκB activity in MS culture, MS were allowed to form over 7 days and inhibitors were added for the last 3 or 6 hours of culture. IKK7, a known IKKα/β inhibitor, was used as a positive control. MS displayed elevated levels of p65 DNA binding activity (Fig. 3A) and high NFκB target gene expression (Fig. 3B) compared to untreated breast cancer cells cultured in standard monolayer (2D) conditions. All of these endpoints were attenuated by DMF or IKK7 to the same extent (Fig. 3A, 3B), suggesting that DMF can abrogate MS formation by inhibiting the NFκB pathway.

Besides NFκB inhibition, DMF has also been proposed to activate Nrf2 (23-26). Indeed, we find DMF significantly upregulates the Nrf2 target gene, heme oxygenase 1 (HMOX1) mRNA, both in 2D and in MS (Fig. 3C). However, an alternative Nrf2 activator, Compound 16 (39), does not inhibit MS formation (Fig. 3E), indicating Nrf2 activation is not likely to contribute to DMF's inhibitory activity in MS.

*DMF Blocks p65 DNA Binding, its Transcriptional Activity, and its Nuclear Translocation* – To determine where in the NFκB pathway DMF may be acting, we first examined DNA binding activity of the main NFκB family member, p65 (RelA) upon TNFα induced activation in MCF-7 cells. DMF attenuates p65 DNA binding by ~50%, which is comparable in this assay to the known IKK α/β inhibitor, IKK7 (Fig. 4A). We next examined DMF's effect on TNFα-induced p65 DNA recruitment and occupancy on the promoters of the NFκB target genes, ICAM1 and CCL2, via a chromatin immunoprecipitation (ChIP) assay. We find that DMF significantly reduces p65 occupancy on both gene promoters (Fig. 4B), indicating that DMF inhibits p65 transcriptional activity. Interestingly, we also find that total and phosphorylated p65 nuclear protein levels are reduced to the same extent upon treatment, suggesting DMF exerts its effect on p65 independently of phosphorylation status. (Fig. 4C, 4D). This observation is corroborated by IHC studies where DMF significantly prevents p65 nuclear localization upon TNFα activation (Fig. 4E, 4F). However,

cellular content of upstream components in the NFκB signaling pathway, such as IKKα/β phosphorylation, IκBα phosphorylation and degradation, and p65 phosphorylation, are not affected by DMF. In contrast, IKK7 reduces the nuclear levels of phosphorylated and total p65 similarly to DMF (Fig. 4C), and also significantly attenuates upstream NFκB signaling as indicated in Fig. 4G, consistent with its known inhibitory effect on IKKα/β. This suggests that DMF's inhibitory action on p65 nuclear localization and its transcriptional activity is mediated by a target downstream of IKK/IκBα.

*DMF Inhibits NFκB by Direct Covalent Modification of p65* – DMF is a cell permeable α,β-unsaturated electrophilic Michael acceptor that can covalently react with reactive cellular nucleophiles, notably protein cysteine residues (40,41). First, to determine whether the fumarate Michael acceptor is responsible for activity, we tested dimethyl succinate (DMS), the saturated analog of DMF devoid of the fumarate's double bond, hence unable to form covalent protein adducts. We find that DMS at 20μM (corresponding to the IC<sub>50</sub> of DMF) is unable to inhibit the NFκB pathway in MCF-7 cells (Fig. 5A, 5B). This indicates that the electrophilic reactivity associated with the double bond of fumarate is required for DMF's anti-NFκB activity. Secondly, to trap DMF before reaction with protein cysteine residues, we utilized the cell-permeable small molecule thiol, N-acetyl L-cysteine (NAC) that will react directly with DMF. Pre-treatment of cells with NAC reverses DMF's inhibition of NFκB target genes (Fig. 5C solid line), further supporting the notion that the activity of DMF is caused by covalent modification of a cellular target.

Thus far, the data obtained from using DMS and NAC indicates that fumarate's electrophilic reactivity, and hence its ability to form covalent protein adducts, drives DMF's anti-NFκB activity. As presented above, our data indicates that the inhibition of p65 activity by DMF is mediated by a protein target downstream of IKK/IκBα. That p65 may be directly targeted by DMF, is supported by the fact that p65 contains numerous reactive cysteines susceptible to covalent modification by electrophiles (32,42-45). Thus, we asked whether DMF's effect on p65

activity is the result of direct inactivation as opposed to an indirect effect. To test this, we pre-incubated recombinant p65 protein with DMF and observed a significant attenuation of p65 DNA binding activity, indicating a direct interaction between p65 and DMF (Fig. 6A). Based on our data and the nature of DMF, we hypothesized that DMF inhibits the NFκB pathway via direct covalent modification of p65 cysteine residues. To test this hypothesis, we synthesized a novel chemical probe of DMF shown in Fig. 6B, designed to replicate the biological activity of DMF. The small alkynyl modification to DMF is designed to allow visualization and immunoprecipitation (IP) of covalently modified proteins, without loss or deviation of the specific bioactivity of DMF (35). We find that the alkynyl-DMF probe recapitulates the inhibitory activity of DMF on classical NFκB target genes, such as TNF and CCL2 (Fig. 6C). The probe was then incubated with recombinant p65 protein, followed by “click chemistry” crosslinking to the azido-rhodamine reporter tag using copper-catalyzed cycloaddition (36). The probe-labelled p65 protein was then visualized by SDS-PAGE using in-gel fluorescence scanning (35) as shown in Fig. 6D, indicating a significant labelling of p65 (second lane). Pre-incubation of p65 with DMF before addition of alkynyl-DMF probe reduces p65 labelling by the probe, indicating that DMF and probe compete for and covalently modify the same site on p65. These data show that DMF covalently modifies recombinant p65. To determine whether this finding also applies to breast cancer cells, MDA-MB-231 cell lysates were incubated with alkynyl-DMF probe, and in this experiment, crosslinked by “click chemistry” to an azido-biotin reporter tag, allowing IP using streptavidin beads to capture biotinylated-protein. Cell lysates prior to IP showed significant levels of p65 using an antibody for p65 (Fig. 6E, first two lanes). The eluate from streptavidin bead IP also showed significant alkynyl-DMF modified p65 (Fig. 6E, third lane). The control experiment in which the alkynyl-DMF probe was omitted from the experiment, showed no p65 protein from the eluate after IP (Fig. 6E, last lane). Altogether, the data demonstrate that DMF covalently modifies p65 both recombinant protein and in cell lysates.

The transcription factor p65 has multiple reactive cysteines (46,47), but in particular

cysteine 38 (C38) has been shown to be alkylated by electrophiles similar in nature to DMF (32,42-45). Because C38 participates in DNA binding of p65 (42,48), and because its covalent modification was shown to inhibit p65 nuclear localization (43), we examined whether DMF's action was dependent on C38 covalent modification by expressing wild type p65 or C38S-p65. In the mutant, the thiol functional group is replaced by an alcohol, which can no longer react with DMF. We find that the transfected cells overexpressing wild type or C38S mutant exhibit elevated p65 activity measured by NFκB-RE luciferase and no stimulation by TNFα is needed (Fig. 6F). DMF treatment significantly reduced wild type p65 activity; however, C38S activity is significantly less inhibited by DMF (Fig. 6G). This data demonstrates that cysteine 38 is a key residue mediating DMF's effect on p65 activity.

## **DISCUSSION**

In this study, we have demonstrated that DMF can be effectively used to inhibit NFκB activity in breast cancer cells. Importantly, we showed that DMF attenuates MS formation by inhibiting their intrinsic high NFκB activity. This indicates that DMF's anti-NFκB activity can be exploited to eradicate breast CSCs, given their reliance on the NFκB pathway for survival and propagation, making DMF a candidate for anti-CSC therapy in breast cancer. This is in agreement with our prior findings that fumarate-based drugs are effective anti-breast CSC agents (49).

Similarly, one can envision that DMF may have additional anti-tumor activities by inhibiting other NFκB-dependent phenotypes, such as tumor cell proliferation and survival. Indeed, we demonstrate that DMF significantly impaired the growth of MDA-MB-231 xenograft tumors. Because the MDA-MB-231 cells represent the aggressive triple negative breast cancer subtype, this is highly significant. Triple negative breast cancers have aggressive clinical manifestations, lack targeted therapy, and as a result, patient outcome remains poor. Furthermore, the triple negative subtype is enriched with CSC markers more than other subtypes (50), and displays higher NFκB activity (51), suggesting that application of DMF therapy may be highly beneficial.

Although DMF is an approved immunomodulatory drug that has been shown to inhibit NFκB signaling in a variety of cell lines and tissues (23-26,52), the activity in breast cancer cells was unknown and the specific mechanism of action with respect to the NFκB pathway was unclear. Previous reports had suggested that upon DMF treatment, phosphorylation of NFκB transcription factors and subsequent nuclear translocation are attenuated (26,52); this occurs in an IKK/IκBα independent manner and via other kinases such as MSK-1, which phosphorylates p65 at Ser468 (24,26,52). In agreement with these reports, we find that in breast cancer cells DMF reduces nuclear content of phosphorylated and total p65 in an IKK/IκBα independent manner. However, when examining cellular content of phosphorylated p65 including the Ser468 site, no change is observed, suggesting that a kinase-mediated effect on p65 is unlikely in breast cancer cells, at least at the concentration used in our study (50μM DMF versus 100μM in Peng et al. study (26,52)). Instead, our data demonstrate that DMF inhibits NFκB activity in breast cancer cells by covalently modifying the main transcription factor of the NFκB family, p65 on cysteine 38, which in turn blocks p65 nuclear translocation and DNA binding activity.

Reactive protein cysteine residues are expected to be modified by DMF, as they are the most intrinsically nucleophilic amino acid in proteins. The p65 transcription factor has multiple such cysteines – a total of nine cysteine residues are clustered in the Rel domain and six of them are highly conserved among all other known Rel-related proteins (46,47). In particular cysteines C38 and C120 have been shown to be alkylated by electrophiles similar in nature to DMF (32,42-45). Our results show more than one modification site as indicated in Fig. 6E, consistent with multiple reactive cysteine residues in p65. Intriguingly, C38 participates in DNA binding of p65 by forming a hydrogen bond with the sugar/phosphate DNA backbone (42,48). Moreover, covalent modification of C38 was shown to inhibit the nuclear localization of p65 (43). Thus p65 C38 alkylation may contribute to attenuate NFκB activity in breast cancer cells, suggesting this may be the main mode of action for DMF. In this paper we use the point mutant to prove that C38 of p65

is a key amino acid required for DMF-mediated NFκB inhibition in breast cancer cells.

Drugs that are covalent inhibitors, like DMF, exhibit multiple advantages over conventional non-covalent drugs such as: (i) improved biochemical efficiency as competition with endogenous substrates is reduced, (ii) lower, less frequent dosing resulting in a lower overall patient burden, and (iii) potential prevention of drug resistance due to continuous target suppression (53). Determining DMF's mechanism of action is important because it may enable: (i) to better dose through monitoring of the drug's effects on the target pathway in patients, (ii) to

predict potential side effects, and (iii) to stratify clinical trials to focus on patients most likely to respond. Altogether, we conclude that DMF represents an effective way to inhibit NFκB in breast cancer cells. Furthermore, we demonstrate that DMF has anti-tumor activity in a breast cancer xenograft model of triple negative subtype. Our findings have a tremendous clinical impact by establishing DMF as a viable NFκB inhibitor, an anti-CSC and anti-tumor agent. By understanding DMF's mechanism of action, it sets the stage for advancing DMF into clinical testing to treat aggressive breast cancers.

**Acknowledgements** – This work was supported by grants provided by the National Institutes of Health (NIH), R01 CA130932 and R01 CA200669 to JF, R01 CA121107 to GRJT, and by a postdoctoral fellowship grant from Susan G. Komen for the Cure to IK (PDF12229484). We thank Dr. Thomas Gilmore for providing the wild type and mutant p65 plasmids. We thank Shuangping Zhao, Bryant Marure, Jeanne Danes, Ye Li, and Daniel D. Lantvit for technical assistance.

**Conflict of Interest** – The authors declare that they have no conflicts of interest with the contents of this article.

**Author Contributions** – IK conceived and coordinated the study, performed and analyzed most of the experiments, and wrote the paper. MIS synthesized the alkynyl-DMF probe shown in Figure 6B. ELCG performed the daily gavage and assisted in the animal study data collection. LES performed the IHC staining shown in Figure 4E. GG performed the dual luciferase assay shown in Figure 6F and 6G and assisted with the crystal violet assay shown in Figure 3B. ENT optimized the click chemistry procedure shown in Figure 6D. GRJT and JF contributed to the preparation of the figures and drafting of the paper. All authors reviewed the results and approved the final version of the manuscript.

**Abbreviations** – CSC, cancer stem cells; C, cysteine; DMF, dimethyl fumarate; DMS, dimethyl succinate; MS, mammosphere; NAC, N-acetyl L-cysteine; NFκB, nuclear factor κB.

## REFERENCES

1. Hanahan, D., and Weinberg, R. A. (2011) Hallmarks of cancer: the next generation. *Cell* **144**, 646-674
2. Baumgarten, S. C., and Frasor, J. (2012) Inflammation: an instigator of more aggressive estrogen receptor (ER) positive breast cancers. *Mol. Endocrinol.* **26**, 360-371
3. Karin, M., Cao, Y., Greten, F. R., and Li, Z. W. (2002) NF-kappaB in cancer: from innocent bystander to major culprit. *Nat. Rev. Cancer* **2**, 301-310
4. Kim, H. J., Hawke, N., and Baldwin, A. S. (2006) NF-kappaB and IKK as therapeutic targets in cancer. *Cell Death Differ.* **13**, 738-747
5. Nakshatri, H., Bhat-Nakshatri, P., Martin, D. A., Goulet, R. J., Jr., and Sledge, G. W., Jr. (1997) Constitutive activation of NF-kappaB during progression of breast cancer to hormone-independent growth. *Mol. Cell. Biol.* **17**, 3629-3639
6. Sovak, M. A., Bellas, R. E., Kim, D. W., Zanieski, G. J., Rogers, A. E., Traish, A. M., and Sonenshein, G. E. (1997) Aberrant nuclear factor-kappaB/Rel expression and the pathogenesis of breast cancer. *J. Clin. Invest.* **100**, 2952-2960

7. Nakshatri, H., and Goulet, R. J., Jr. (2002) NF-kappaB and breast cancer. *Curr. Probl. Cancer* **26**, 282-309
8. Zhou, Y., Eppenberger-Castori, S., Marx, C., Yau, C., Scott, G. K., Eppenberger, U., and Benz, C. C. (2005) Activation of nuclear factor-kappaB (NFkappaB) identifies a high-risk subset of hormone-dependent breast cancers. *Int. J. Biochem. Cell Biol.* **37**, 1130-1144
9. Jones, R. L., Rojo, F., A'Hern, R., Villena, N., Salter, J., Corominas, J. M., Servitja, S., Smith, I. E., Rovira, A., Reis-Filho, J. S., Dowsett, M., and Albanell, J. (2011) Nuclear NF-kappaB/p65 expression and response to neoadjuvant chemotherapy in breast cancer. *J. Clin. Pathol.* **64**, 130-135
10. Cao, Y., Luo, J. L., and Karin, M. (2007) IkappaB kinase alpha kinase activity is required for self-renewal of ErbB2/Her2-transformed mammary tumor-initiating cells. *Proc. Natl. Acad. Sci. U. S. A.* **104**, 15852-15857
11. Iliopoulos, D., Hirsch, H. A., and Struhl, K. (2009) An epigenetic switch involving NF-kappaB, Lin28, Let-7 MicroRNA, and IL6 links inflammation to cell transformation. *Cell* **139**, 693-706
12. Hinohara, K., Kobayashi, S., Kanauchi, H., Shimizu, S., Nishioka, K., Tsuji, E., Tada, K., Umezawa, K., Mori, M., Ogawa, T., Inoue, J., Tojo, A., and Gotoh, N. (2012) ErbB receptor tyrosine kinase/NF-kappaB signaling controls mammosphere formation in human breast cancer. *Proc. Natl. Acad. Sci. U. S. A.* **109**, 6584-6589
13. Al-Hajj, M., Wicha, M. S., Benito-Hernandez, A., Morrison, S. J., and Clarke, M. F. (2003) Prospective identification of tumorigenic breast cancer cells. *Proc. Natl. Acad. Sci. U. S. A.* **100**, 3983-3988
14. Li, X., Lewis, M. T., Huang, J., Gutierrez, C., Osborne, C. K., Wu, M. F., Hilsenbeck, S. G., Pavlick, A., Zhang, X., Chamness, G. C., Wong, H., Rosen, J., and Chang, J. C. (2008) Intrinsic resistance of tumorigenic breast cancer cells to chemotherapy. *J. Natl. Cancer Inst.* **100**, 672-679
15. Croker, A. K., and Allan, A. L. (2008) Cancer stem cells: implications for the progression and treatment of metastatic disease. *J. Cell. Mol. Med.* **12**, 374-390
16. Hollier, B. G., Evans, K., and Mani, S. A. (2009) The epithelial-to-mesenchymal transition and cancer stem cells: a coalition against cancer therapies. *J. Mammary Gland Biol. Neoplasia* **14**, 29-43
17. Diehn, M., Cho, R. W., Lobo, N. A., Kalisky, T., Dorie, M. J., Kulp, A. N., Qian, D., Lam, J. S., Ailles, L. E., Wong, M., Joshua, B., Kaplan, M. J., Wapnir, I., Dirbas, F. M., Somlo, G., Garberoglio, C., Paz, B., Shen, J., Lau, S. K., Quake, S. R., Brown, J. M., Weissman, I. L., and Clarke, M. F. (2009) Association of reactive oxygen species levels and radioresistance in cancer stem cells. *Nature* **458**, 780-783
18. Velasco-Velazquez, M. A., Popov, V. M., Lisanti, M. P., and Pestell, R. G. (2011) The role of breast cancer stem cells in metastasis and therapeutic implications. *Am. J. Pathol.* **179**, 2-11
19. Gilmore, T. D., and Herscovitch, M. (2006) Inhibitors of NF-kappaB signaling: 785 and counting. *Oncogene* **25**, 6887-6899
20. Hayden, M. S., and Ghosh, S. (2008) Shared principles in NF-kappaB signaling. *Cell* **132**, 344-362
21. Garber, K. (2006) The second wave in kinase cancer drugs. *Nat. Biotechnol.* **24**, 127-130
22. Greten, F. R., Arkan, M. C., Bollrath, J., Hsu, L. C., Goode, J., Miething, C., Goktuna, S. I., Neuenhahn, M., Fierer, J., Paxian, S., Van Rooijen, N., Xu, Y., O'Cain, T., Jaffee, B. B., Busch, D. H., Duyster, J., Schmid, R. M., Eckmann, L., and Karin, M. (2007) NF-kappaB is a negative regulator of IL-1beta secretion as revealed by genetic and pharmacological inhibition of IKKbeta. *Cell* **130**, 918-931
23. Vandermeeren, M., Janssens, S., Wouters, H., Borghmans, I., Borgers, M., Beyaert, R., and Geysen, J. (2001) Dimethylfumarate is an inhibitor of cytokine-induced nuclear translocation of NF-kappa B1, but not RelA in normal human dermal fibroblast cells. *J. Invest. Dermatol.* **116**, 124-130

24. Seidel, P., Merfort, I., Hughes, J. M., Oliver, B. G., Tamm, M., and Roth, M. (2009) Dimethylfumarate inhibits NF-κB function at multiple levels to limit airway smooth muscle cell cytokine secretion. *Am. J. Physiol. Lung Cell Mol. Physiol.* **297**, L326-339
25. Wilms, H., Sievers, J., Rickert, U., Rostami-Yazdi, M., Mrowietz, U., and Lucius, R. (2010) Dimethylfumarate inhibits microglial and astrocytic inflammation by suppressing the synthesis of nitric oxide, IL-1β, TNF-α and IL-6 in an in-vitro model of brain inflammation. *J. Neuroinflammation* **7**, 30
26. Peng, H., Guerau-de-Arellano, M., Mehta, V. B., Yang, Y., Huss, D. J., Papenfuss, T. L., Lovett-Racke, A. E., and Racke, M. K. (2012) Dimethyl fumarate inhibits dendritic cell maturation via nuclear factor κB (NF-κB) and extracellular signal-regulated kinase 1 and 2 (ERK1/2) and mitogen stress-activated kinase 1 (MSK1) signaling. *J. Biol. Chem.* **287**, 28017-28026
27. Hoefnagel, J. J., Thio, H. B., Willemze, R., and Bouwes Bavinck, J. N. (2003) Long-term safety aspects of systemic therapy with fumaric acid esters in severe psoriasis. *Br. J. Dermatol.* **149**, 363-369
28. Gotz, M. G., James, K. E., Hansell, E., Dvorak, J., Seshadri, A., Sojka, D., Kopacek, P., McKerrow, J. H., Caffrey, C. R., and Powers, J. C. (2008) Aza-peptidyl Michael acceptors. A new class of potent and selective inhibitors of asparaginyl endopeptidases (legumains) from evolutionarily diverse pathogens. *J. Med. Chem.* **51**, 2816-2832
29. Mercurio, F., Zhu, H., Murray, B. W., Shevchenko, A., Bennett, B. L., Li, J., Young, D. B., Barbosa, M., Mann, M., Manning, A., and Rao, A. (1997) IKK-1 and IKK-2: cytokine-activated IκB kinases essential for NF-κB activation. *Science* **278**, 860-866
30. Kastrati, I., Canestrari, E., and Frasar, J. (2015) PHLDA1 expression is controlled by an estrogen receptor-NFκB-miR-181 regulatory loop and is essential for formation of ER+ mammospheres. *Oncogene* **34**, 2309-2316.
31. Pradhan, M., Baumgarten, S. C., Bembinster, L. A., and Frasar, J. (2012) CBP mediates NF-κB-dependent histone acetylation and estrogen receptor recruitment to an estrogen response element in the BIRC3 promoter. *Mol. Cell. Biol.* **32**, 569-575
32. Liang, M. C., Bardhan, S., Pace, E. A., Rosman, D., Beutler, J. A., Porco, J. A., Jr., and Gilmore, T. D. (2006) Inhibition of transcription factor NF-κB signaling proteins IKKβ and p65 through specific cysteine residues by epoxyquinone A monomer: correlation with its anti-cancer cell growth activity. *Biochem. Pharmacol.* **71**, 634-645
33. Frasar, J., Danes, J. M., Komm, B., Chang, K. C., Lyttle, C. R., and Katzenellenbogen, B. S. (2003) Profiling of estrogen up- and down-regulated gene expression in human breast cancer cells: insights into gene networks and pathways underlying estrogenic control of proliferation and cell phenotype. *Endocrinology* **144**, 4562-4574
34. Stender, J. D., Kim, K., Charn, T. H., Komm, B., Chang, K. C., Kraus, W. L., Benner, C., Glass, C. K., and Katzenellenbogen, B. S. (2010) Genome-wide analysis of estrogen receptor alpha DNA binding and tethering mechanisms identifies Runx1 as a novel tethering factor in receptor-mediated transcriptional activation. *Mol. Cell. Biol.* **30**, 3943-3955
35. Speers, A. E., Adam, G. C., and Cravatt, B. F. (2003) Activity-based protein profiling in vivo using a copper(i)-catalyzed azide-alkyne [3 + 2] cycloaddition. *J Am. Chem. Soc.* **125**, 4686-4687
36. Rostovtsev, V. V., Green, L. G., Fokin, V. V., and Sharpless, K. B. (2002) A stepwise Huisgen cycloaddition process: copper(I)-catalyzed regioselective "ligation" of azides and terminal alkynes. *Angew. Chem.* **41**, 2596-2599
37. Dontu, G., Abdallah, W. M., Foley, J. M., Jackson, K. W., Clarke, M. F., Kawamura, M. J., and Wicha, M. S. (2003) In vitro propagation and transcriptional profiling of human mammary stem/progenitor cells. *Genes Dev.* **17**, 1253-1270
38. Charafe-Jauffret, E., Monville, F., Ginestier, C., Dontu, G., Birnbaum, D., and Wicha, M. S. (2008) Cancer stem cells in breast: current opinion and future challenges. *Pathobiology* **75**, 75-84
39. Marcotte, D., Zeng, W., Hus, J. C., McKenzie, A., Hession, C., Jin, P., Bergeron, C., Lugovskoy, A., Enyedy, I., Cuervo, H., Wang, D., Atmanene, C., Roecklin, D., Vecchi, M., Vivat, V.,

- Kraemer, J., Winkler, D., Hong, V., Chao, J., Lukashev, M., and Silvan, L. (2013) Small molecules inhibit the interaction of Nrf2 and the Keap1 Kelch domain through a non-covalent mechanism. *Bioorg. Med. Chem* **21**, 4011-4019
40. Linker, R. A., Lee, D. H., Ryan, S., van Dam, A. M., Conrad, R., Bista, P., Zeng, W., Hronowsky, X., Buko, A., Chollate, S., Ellrichmann, G., Bruck, W., Dawson, K., Goelz, S., Wiese, S., Scannevin, R. H., Lukashev, M., and Gold, R. (2011) Fumaric acid esters exert neuroprotective effects in neuroinflammation via activation of the Nrf2 antioxidant pathway. *Brain* **134**, 678-692
  41. Sullivan, L. B., Martinez-Garcia, E., Nguyen, H., Mullen, A. R., Dufour, E., Sudarshan, S., Licht, J. D., Deberardinis, R. J., and Chandel, N. S. (2013) The proto-oncometabolite fumarate binds glutathione to amplify ROS-dependent signaling. *Mol. Cell* **51**, 236-248
  42. Garcia-Pineros, A. J., Castro, V., Mora, G., Schmidt, T. J., Strunck, E., Pahl, H. L., and Merfort, I. (2001) Cysteine 38 in p65/NF-kappaB plays a crucial role in DNA binding inhibition by sesquiterpene lactones. *J. Biol. Chem.* **276**, 39713-39720
  43. Tamura, R., Morimoto, K., Hirano, S., Wang, L., Zhao, M., Ando, M., and Kataoka, T. (2012) Santonin-related compound 2 inhibits the nuclear translocation of NF-kappaB subunit p65 by targeting cysteine 38 in TNF-alpha-induced NF-kappaB signaling pathway. *Biosci. Biotechnol. Biochem* **76**, 2360-2363
  44. Yamamoto, M., Horie, R., Takeiri, M., Kozawa, I., and Umezawa, K. (2008) Inactivation of NF-kappaB components by covalent binding of (-)-dehydroxymethylepoxyquinomicin to specific cysteine residues. *J. Med. Chem.* **51**, 5780-5788
  45. Anand, P., Kunnumakkara, A. B., Harikumar, K. B., Ahn, K. S., Badmaev, V., and Aggarwal, B. B. (2008) Modification of cysteine residue in p65 subunit of nuclear factor-kappaB (NF-kappaB) by picroliv suppresses NF-kappaB-regulated gene products and potentiates apoptosis. *Cancer Res.* **68**, 8861-8870
  46. Gilmore, T. D. (1990) NF-kappa B, KBF1, dorsal, and related matters. *Cell* **62**, 841-843
  47. Ruben, S. M., Dillon, P. J., Schreck, R., Henkel, T., Chen, C. H., Maher, M., Baeuerle, P. A., and Rosen, C. A. (1991) Isolation of a rel-related human cDNA that potentially encodes the 65-kD subunit of NF-kappa B. *Science* **251**, 1490-1493
  48. Chen, F. E., Huang, D. B., Chen, Y. Q., and Ghosh, G. (1998) Crystal structure of p50/p65 heterodimer of transcription factor NF-kappaB bound to DNA. *Nature* **391**, 410-413
  49. Kastrati, I., Litosh, V. A., Zhao, S., Alvarez, M., Thatcher, G. R., and Frasor, J. (2015) A novel aspirin prodrug inhibits NFkappaB activity and breast cancer stem cell properties. *BMC Cancer* **15**, 845
  50. Herschkowitz, J. I., Zhao, W., Zhang, M., Usary, J., Murrow, G., Edwards, D., Knezevic, J., Greene, S. B., Darr, D., Troester, M. A., Hilsenbeck, S. G., Medina, D., Perou, C. M., and Rosen, J. M. (2012) Comparative oncogenomics identifies breast tumors enriched in functional tumor-initiating cells. *Proc. Natl. Acad. Sci. U. S. A.* **109**, 2778-2783
  51. Nakshatri, H., Bhat-Nakshatri, P., Martin, D. A., Goulet, R. J., Jr., and Sledge, G. W., Jr. (1997) Constitutive activation of NF-kappaB during progression of breast cancer to hormone-independent growth. *Mol. Cell. Biol.* **17**, 3629-3639
  52. Loewe, R., Holnthoner, W., Groger, M., Pillinger, M., Gruber, F., Mechtcheriakova, D., Hofer, E., Wolff, K., and Petzelbauer, P. (2002) Dimethylfumarate inhibits TNF-induced nuclear entry of NF-kappa B/p65 in human endothelial cells. *J. Immunol.* **168**, 4781-4787
  53. Mah, R., Thomas, J. R., and Shafer, C. M. (2014) Drug discovery considerations in the development of covalent inhibitors. *Bioorg. Med. Chem. Lett.* **24**, 33-39

## FIGURE LEGENDS

**FIGURE 1.** DMF inhibits TNFα-induced and constitutively active NFκB activity in breast cancer cells. *A*, NFκB-RE activity was measured in MCF-7 cells following TNFα (10ng/mL) treatment for 4 hours. *B-D*, Expression of NFκB target genes, TNF and CCL2, following TNFα treatment for 2 hours, was measured by RT-QPCR in MCF-7 cells (*B*), BT474 cells (*C*), and MDA-MB-231 cells (*D*). Increasing concentrations of DMF were added 2 hours prior to treatment with TNFα, and DMF's inhibitory activity is plotted as % of TNFα alone. *E*, Dox-induced expression of NFκB target genes, TNF and CCL2, measured by RT-QPCR, is shown in CA-IKKβ cells. *F*, DMF inhibits expression of TNF and CCL2 genes in CA-IKKβ cells in a dose-dependent manner. DMF's inhibitory activity is plotted as % of Dox alone. IC<sub>50</sub> values were calculated with the GraphPad software using normalized data. *G*, DMF has no effect on estrogen receptor target genes, TFF1 and IGFBP4 mRNA, measured in MCF-7 cells pre-treated with DMF (20μM) for 2 hours, followed by estrogen treatment (E2, 10nM) for another 2 hours.

**FIGURE 2.** DMF has anti breast cancer activity both in vitro and in vivo. *A*, MS formation (solid line) and 2D cell growth (dashed line) in the indicated cell lines were measured after treatment with varying concentrations of DMF. The effect of DMF is plotted as % of DMSO vehicle control. *B*, Representative pictures at 10X of MCF-7 MS formation upon treatment with DMF or the NFκB inhibitors, IKK7 (5μM) and Bay117082 (Bay, 10μM) are shown. *C*, Effect of DMF (30mg/kg, daily) on MDA-MB-231 xenograft tumor growth is indicated. #, P=0.0002; ##, P=0.003.

**FIGURE 3.** DMF inhibits the intrinsic NFκB activity in MS culture of breast cancer cells. *A*, p65 DNA binding activity was measured via an ELISA in conventional adherent 2D culture of MCF-7 cells or MS culture with or without inhibitors (IKK7 1μM or DMF 50μM) added for the last 3 hours. *B*, Expression of TNF, CCL2, and ICAM1 genes after 6 hours of drug treatment was measured in the same groups described in (*A*). The different letters above bars indicate significant difference between treatments, P<0.001. *C*, DMF (20μM) upregulates expression of HMOX1 mRNA in both 2D and MS of MCF-7 cells. Data shown as fold change compared to Veh control. *D*, Compound 16 (Comp 16, 1μM and 10μM) upregulates expression of HMOX1 mRNA in MCF-7 cells. *E*, MS formation is measured in MCF-7 cells treated with compound 16. \*, P<0.01; \*\*\*, P<0.001.

**FIGURE 4.** DMF inhibits p65 DNA binding and transcriptional activity, and its nuclear translocation in an IKK/IκBα-independent manner. *A*, p65 DNA binding activity was measured in MCF-7 cells treated with IKK7 (1μM) or DMF (50μM) for 2 hours, followed by TNFα treatment for 15 minutes. *B*, ChIP assays were carried out for p65 and IgG control following treatment of MCF-7 cells with TNFα for 45 minutes with or without DMF (50 μM) added 2 hours prior to TNFα. The fold-increase in IgG or p65 occupancy at the ICAM1 (left) and CCL2 (right) promoters were calculated from the percent input of each pulldown and then comparing each treatment to vehicle controls. *C*, Nuclear extracts of cells treated as in (*A*) were prepared and NFκB transcription factors were examined by western blotting. Representative western blots from three independent experiments are shown. TBP served as a loading control. *D*, Densitometry of nuclear proteins relative to TBP is indicated. Data is plotted as % of TNFα alone. *E*, Representative pictures of IHC staining for nuclear p65 in MCF-7 cells treated with DMF (50μM) followed by TNFα for 15 minutes are shown. IHC was performed using an anti-p65 antibody (red) and DAPI (blue) for nuclear staining and visualized using Zeiss Laser scanning microscope. *F*, IHC quantitation for nuclear p65 content in (*E*) is indicated. *G*, Whole cell extracts of cells treated as in (*A*) were prepared and NFκB signaling proteins were examined by western blotting. Representative western blots from three independent experiments are shown. β-actin served as a loading control. The different letters above bars in graphs *A*, *B* and *E* indicate significant difference between treatments, P<0.001.

**FIGURE 5.** DMF's double bond reactivity is required to inhibit the NFκB pathway in breast cancer cells. *A-B*, NFκB-RE activity (*B*) and ICAM1 (*C*) gene expression were measured in MCF-7 cells upon

treatment with DMF or DMS, 20μM each, as described in Fig 1. Data is plotted as % of TNFα alone. The different letters above bars indicate significant difference between treatments, P<0.001. C, NAC (dashed line) reverses DMF's inhibitory effect on the TNFα-induced expression of NFκB target genes, TNF, CCL2, and ICAM1, in MCF-7 cells. NAC (500μM) was added 30 minutes prior to DMF and TNFα treatment.

**FIGURE 6.** DMF covalently modifies p65 both in vitro and in cell lysates, and cysteine 38 is the key residue responsible for DMF's activity on the NFκB pathway. *A*, Recombinant p65 DNA binding activity was measured after incubation with DMF (50μM) for 30 minutes. Data is plotted as % vehicle control. \*\*\*, P<0.001. *B*, The chemical structure of the novel alkyne-based DMF probe is indicated. *C*, Expression of NFκB target genes, TNF and CCL2, in MCF-7 cells was measured by RT-QPCR upon treatment with varying concentrations of DMF probe followed by TNFα. Data is plotted as % of TNFα alone. *D*, Gel image for labelling of recombinant p65 with DMF probe (50μM) measured by in-gel fluorescence. In lane 3, DMF (50μM) was added for 30 minutes prior to incubation with the DMF probe. At the bottom, coomassie staining of the gel indicates equal protein loading. *E*, Biotin immunoprecipitation (IP) is carried out in MDA-MB-231 cell lysates crosslinked in the presence or absence of DMF probe (50μM). Total p65 protein is then immunoblotted and compared between IPs and Inputs (10% of protein lysate load). *F*, NFκB-RE activity was measured in MCF-7 cells transfected with mock, wild type p65 or C38S-p65, and then treated with or without TNFα for 4 hours. *G*, NFκB-RE activity was measured in MCF-7 cells transfected with wild type p65 or C38S-p65 and treated with DMF (50μM). Data is presented as % inhibition relative to Veh control. \*\*\*, P<0.001.

**Figure 1.**

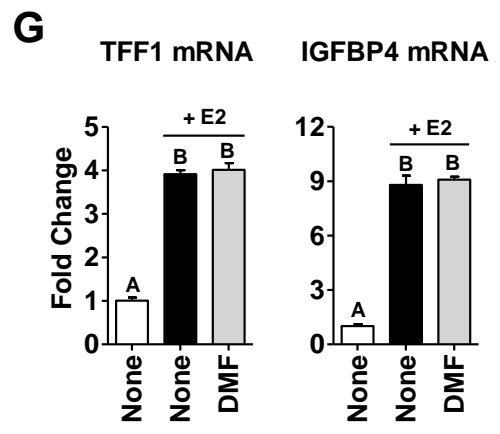
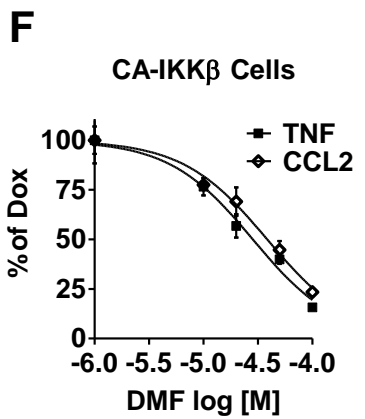
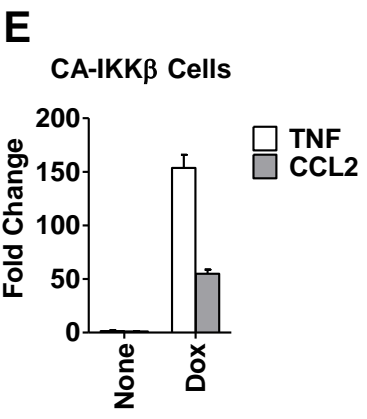
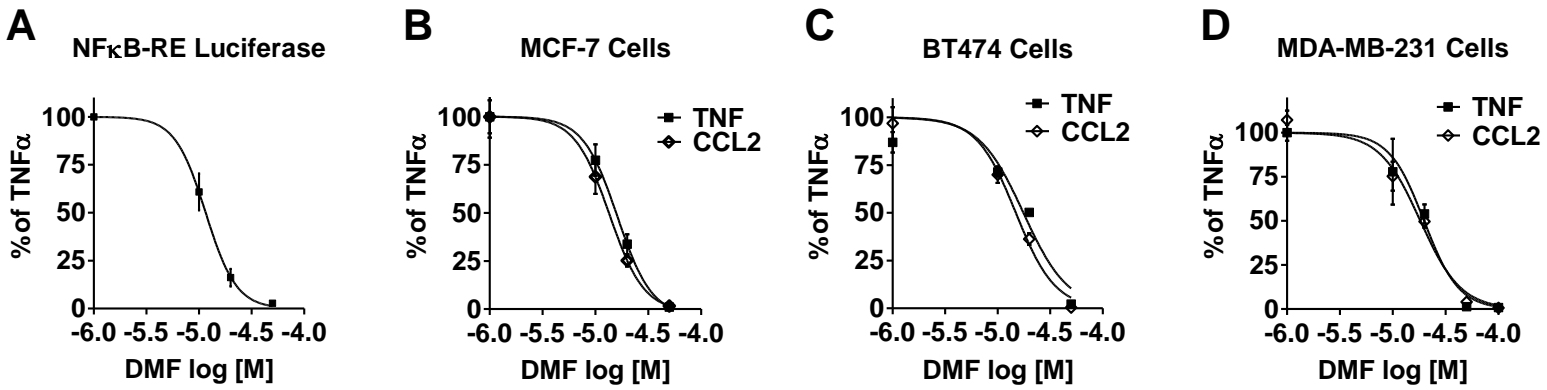


**Figure 2.**

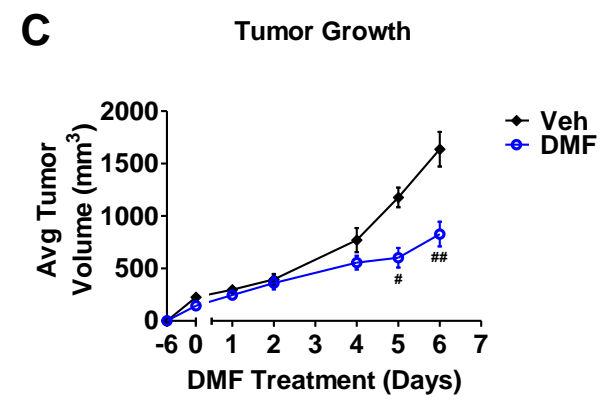
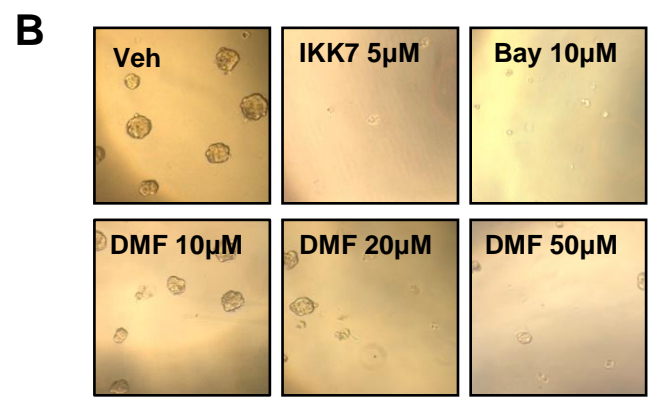
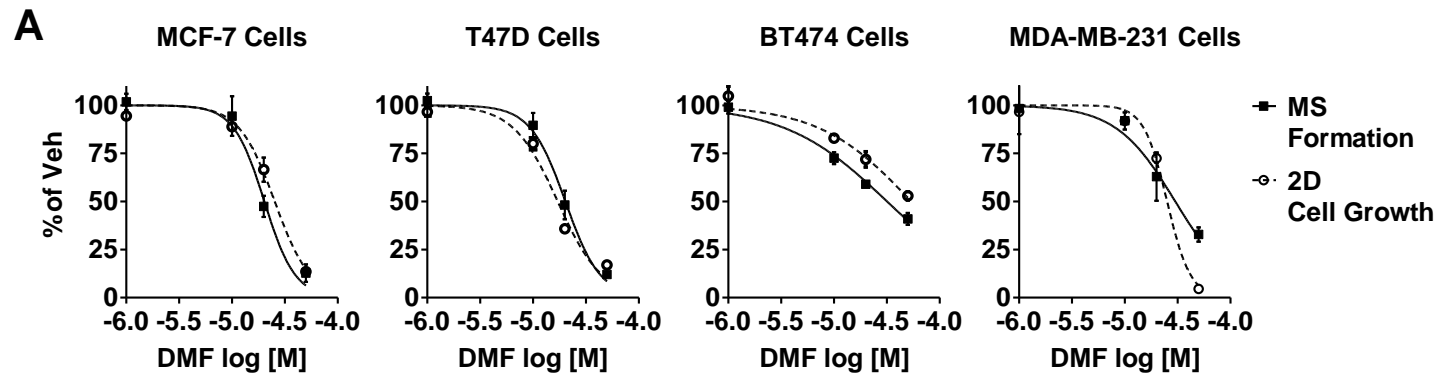


**Figure 3.**

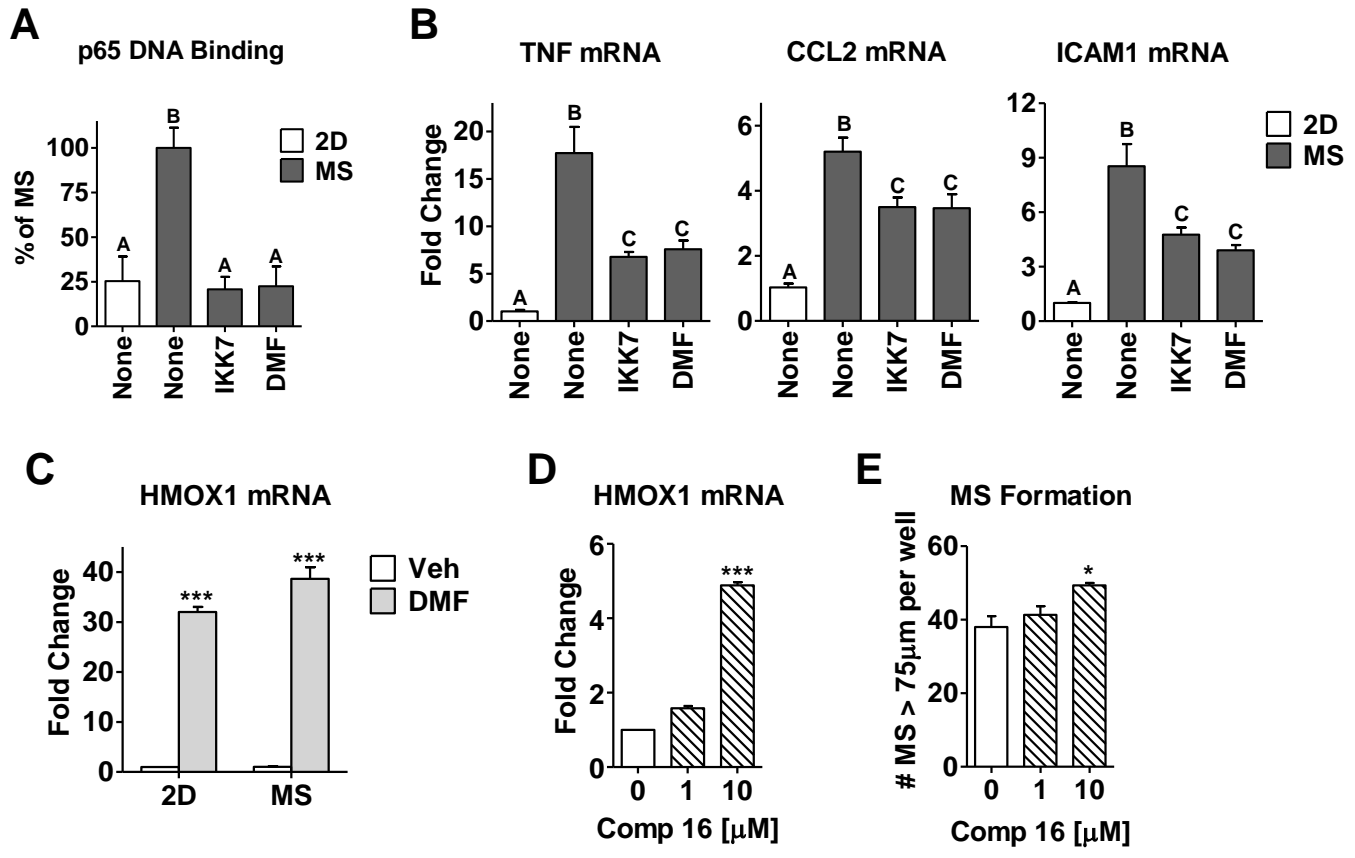


**Figure 4.**

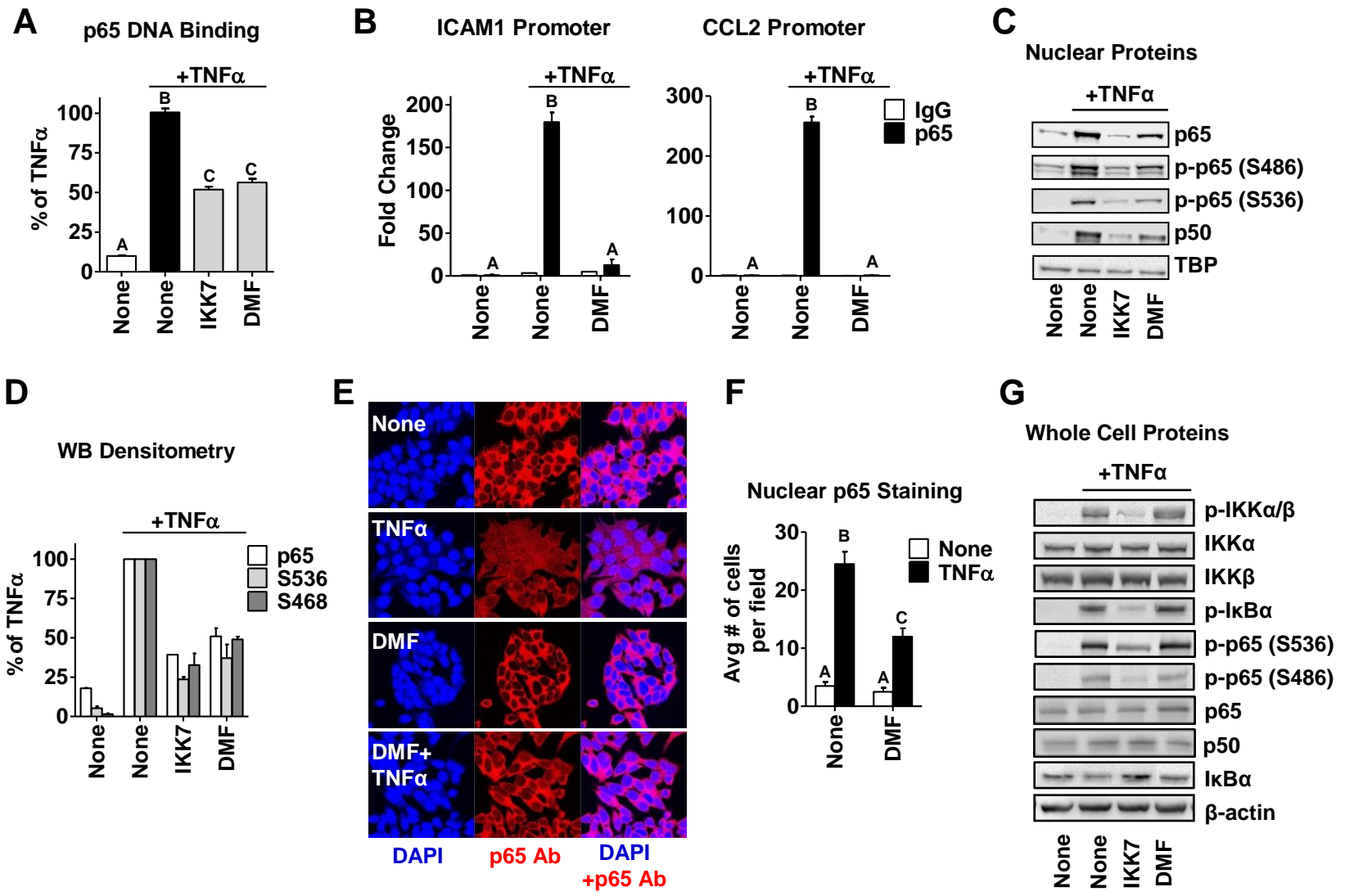
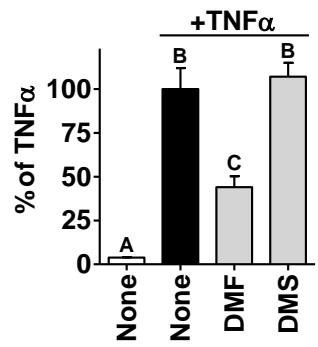
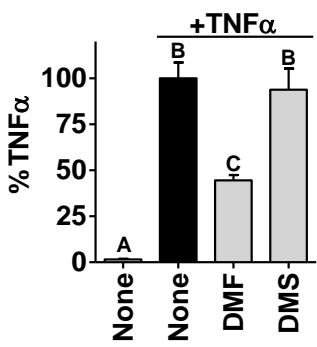


**Figure 5.**

**A** NFκB-RE Activity



**B** ICAM1 mRNA



**C**

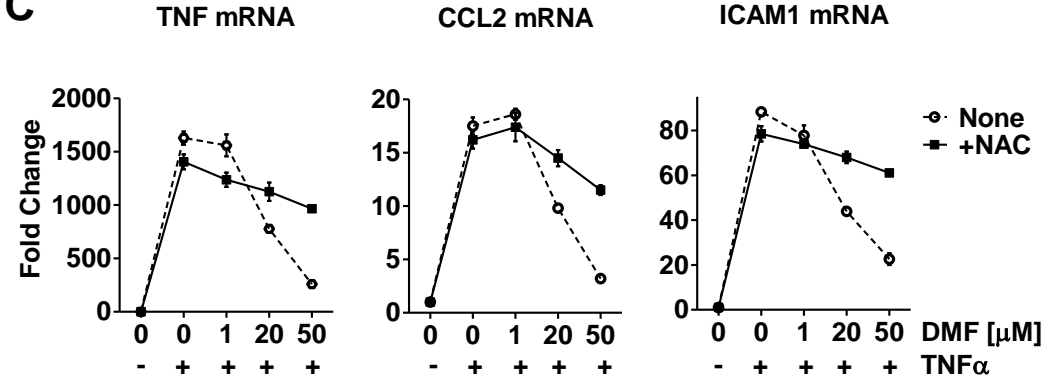
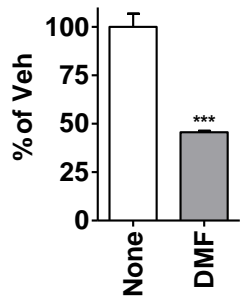


**Figure 6.**

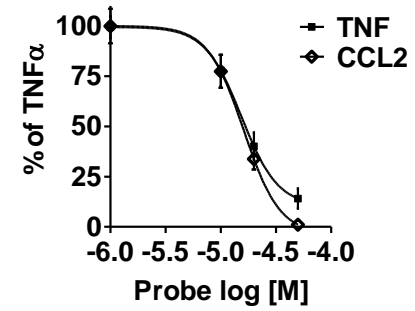
**A** p65 DNA Binding



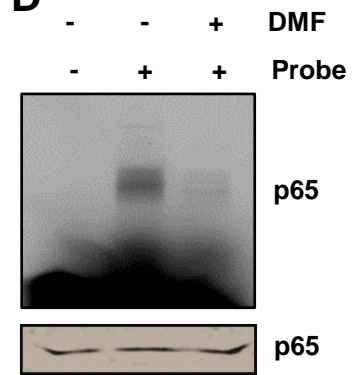
**B**



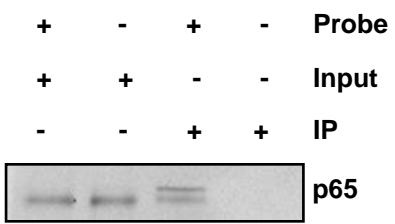
**C**



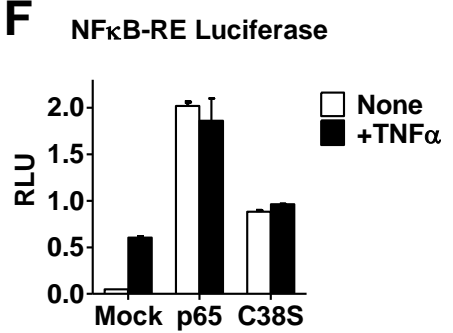
**D**



**E**



**F**



**G**

